

# **Mobility of Radionuclides and Rare Earth Elements in the Coastal area of Rio de Janeiro: Implications for Monazite deposits in Offshore Areas**

**Joney Justo<sup>1</sup>, Valiya M. Hamza<sup>2</sup> and Francisco F. Lamego Simões Filho<sup>3</sup>**

## **Abstract**

Analysis of ground and airborne radiometric data as well as rare earth element abundances in soils in the Saquarema region (Rio de Janeiro, Brazil) has allowed new insights into the mobility of mineral aggregates containing monazites. The regional distributions of radioactive elements, as revealed in results of airborne radiometric surveys, indicate that topography play dominant role in transportation of weathered material. The mobility pattern is characterized by systematic depletion of radioactive elements along the migration paths. Superimposed on this depletion trend are indications of relative enrichment of uranium and thorium with respect to potassium along the migration paths. Analysis of data on rare earth element abundances in soils and beach sands point to the existence of a complementary process responsible for formation of ore-grade deposits of monazites along the coastal regions. The time and distance scales associated with this enrichment process have been estimated based on the regional distribution of Th/K ratios. The results indicate that submerged monazite deposits may be present along the offshore sand banks, in the coastal region of the state of Rio de Janeiro. These results may be useful in locating under-water monazite deposits in other parts of continental shelf with similar geologic context.

**Keywords:** Mobility of Radionuclides, Rare Earths, Rio de Janeiro, Off-shore Deposits

## **1 Introduction**

Knowledge of the distribution of natural radioactive and rare earth elements (REE) in soils is of considerable interest in studies of the dynamics of a variety of geochemical processes occurring in near surface layers [1, 2]. Weathering, in response to environmental conditions near the earth's surface, is often considered to play a significant

---

<sup>1</sup>Department of Geophysics, National Observatory. e-mail: joney@on.br

<sup>2</sup>Department of Geophysics, National Observatory. e-mail: hamza@on.br

<sup>3</sup>Institute of Nuclear Engineering (IEN), e-mail: flamego66@gmail.com

role in the movement of radioactive elements and REE in soil layers [3]. Both naturally radioactive elements and REE appear as natural tracers in the whole geosphere and have become important geochemical tracers during last few decades [4, 5].

The physical and chemical processes associated with weathering of radioactive and rare earth elements have a direct relationship with the break down or alteration of host minerals. Such processes depend primarily on the bonding between the mineral aggregates and the rock matrix undergoing weathering. The mobility of altered material on the land surface is essentially a gravity-driven process, determined primarily by the local topographic conditions. Other factors such as precipitation and the nature of local fluvial systems play secondary roles. The overall result of mobility is distribution of weathered material starting from the source region, which leads to distinct features in the physical and chemical characteristics of soil layers.

A number of studies have been carried out over the last few decades on the distributions of radioactive elements and REE in specific localities in the interior and coastal areas of Brazil [6 – 17]. Nevertheless, few have addressed the problem of distribution patterns of such elements on regional scales, which can provide information on mobility under the combined influence of topography, weathering and erosion. In the present work, we report progress obtained in analysis of airborne radiometric data, with cross-check on selected soil samples, in addressing the problem of mobility of natural radioactive elements and REE. The study area is located in the municipality of Saquarema, in the coastal area of the state of Rio de Janeiro (Brazil). There are indications that the source region of radioactive elements and REE are located in the uplifted crustal blocks of the adjacent Serra do Mar continental escarpment. We examine characteristics in the spatial distribution of these radionuclides and REE and consider its implications for occurrence of eventual ore-grade deposits of Monazites in the adjacent offshore regions. This study does not aim to solve all questions related to the distribution of radioactive elements in the study area but it is of help in obtaining a better understanding of factors affecting their mobility arising from weathering and driven by topography and hydraulic processes at the surface.

## **2 Geologic Context of the Study Area**

The basement rocks in the coastal region southeast Brazil belongs to the Mantiqueira Province. According to geologic studies, the terrain has a number of NE – SW structures composed of thrusts and folds, generated during the Brasiliano Orogeny. The units that constitute the basement rocks are orthogneisses and orthoamphibolites of the Ribeira fold belt of Paleoproterozoic age [18 – 21]. Tectonic processes associated with the opening of the Atlantic have lead to development of extensive escarpments (known as Serra do Mar) along the continental margin areas. Extensive sedimentary layers, of Tertiary to Quaternary age, cover the down-faulted blocks in the coastal area.

The geologic context of the study area (municipality of Saquarema, in the state of Rio de Janeiro) is illustrated in the map of Figure 1. Outcrops of basement rocks in this area are rare as intense weathering processes have led to the formation of thick soil cover. A number of lagoons and backwaters also occur along the coastal region. The climate is sub-tropical with annual median temperatures of 22.5°C and annual median precipitation of 1700 mm and has a long dry season. An understanding of the topographic characteristics is important in evaluating terrain attributes related to geomorphologic processes and soil/regolith properties in the study area. According to the digital elevation map of the study area (see

Figure 2) the escarpments of the highlands (Serra do Mar), along the western border of the study area, have altitudes reaching over 400 meters. It drops rapidly to sea level over distances of approximately 30km.

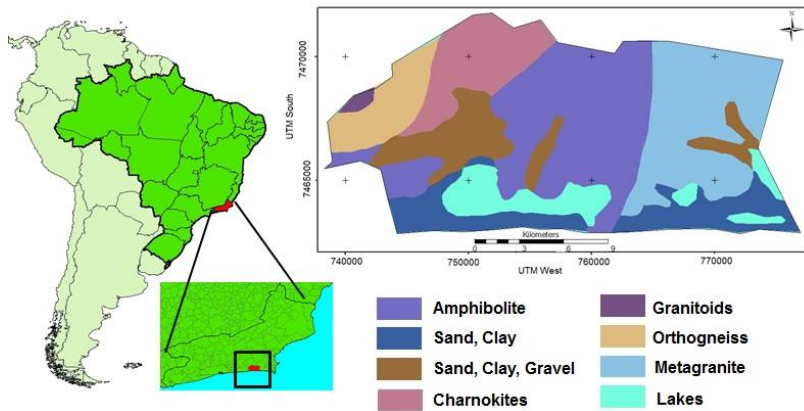


Figure 1: Simplified geologic map of the study area.

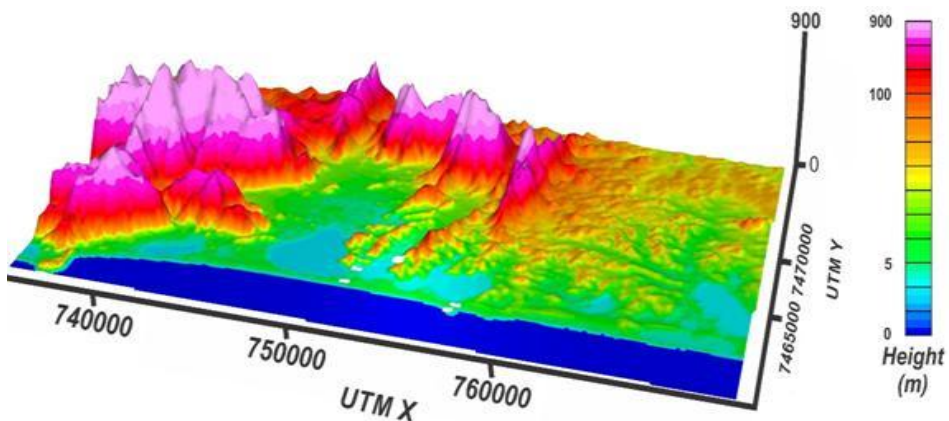


Figure 2: Digital elevation characteristics, with 3D perspectives, of the study area.

### 3 Database

#### 3.1 Airborne Surveys

The results of airborne surveys carried out in 1978, within the framework of the São Paulo – Rio de Janeiro Project [22], were employed in the present work for mapping radioelement abundances in the study area. The data sets available for this survey refer to intensities of gamma ray emissions by natural radioactive elements (potassium, uranium and thorium) at energy levels of 1.46 Mev (million electron-volts), 1.76 Mev and 2.61 Mev respectively. These are recorded in separate channels, along with information on flight altitude and atmospheric conditions. The flight lines were in north – south direction, had a spacing of 1000m and altitude of 150m. Quality control tests were carried out not only prior to data acquisition, but also during and after the surveys. The total investigated area is 654.67km<sup>2</sup>, which includes lakes and lagoons occupying 21.2km<sup>2</sup>.

Most of the data processing in the present work has been carried out using the computational package Geosoft® – Oasis Montag. Initially the raw data were corrected for the perturbing effects of technical survey operations (LAG and Heading effects and altitude variations). In addition, procedures were adopted for filtering, leveling and microleveling operations, as per standard data processing techniques [23]. The original data, recorded in units of counts per second (cps), were transformed into values of relative abundances using conversion factors specific to each flight path. These factors depend on the sensitivity and geometry of detectors used and the survey altitude. The results, corrected using calibration data for the particular survey operations [24 – 26], are reported as equivalent values of thorium (eTh), uranium (eU) and potassium.

The results of airborne survey reveal striking correspondences with geological and morphological features of southeast coastal region in the state of Rio de Janeiro. Consider for example the regional distribution of eTh in the eastern part of the state of Rio de Janeiro (Brazil), illustrated in Figure 3a. The abundances of eTh are relatively high (> 20 ppm) along NE – SW trending belts, which are in remarkable coincidence with exposures of basement rocks along the thrust belts of Brasiliano orogeny. Also, eTh abundances are much lower (< 10 ppm) in the low-lying planes along the coastal region. Similar features are also present in the distribution eU abundances, illustrated in Figure 3b.

Results of regional surveys allow identification of large-scale anomalies, but are not directly useful for investigating the role of topography in determining mobility patterns of radioactive nuclides in the soil layers. In this context, we have used the technique of draping radioelement distributions over 3D representations of the local topographic features, as a convenient method in illustrating features related to variations in elevation. Consider for example the distribution of eU, illustrated in Figure 4. The abundance values of uranium are greater than 3 ppm in areas in the western parts, where altitudes are higher than 100 meters. On the other hand, belts of low concentrations (less than 2ppm) occur in the southern parts of the study area, which have altitudes of less than 10 meters. Lakes and coastal water bodies are present in most such areas. It is clear that there is significant drop in uranium abundances with decrease in elevation.

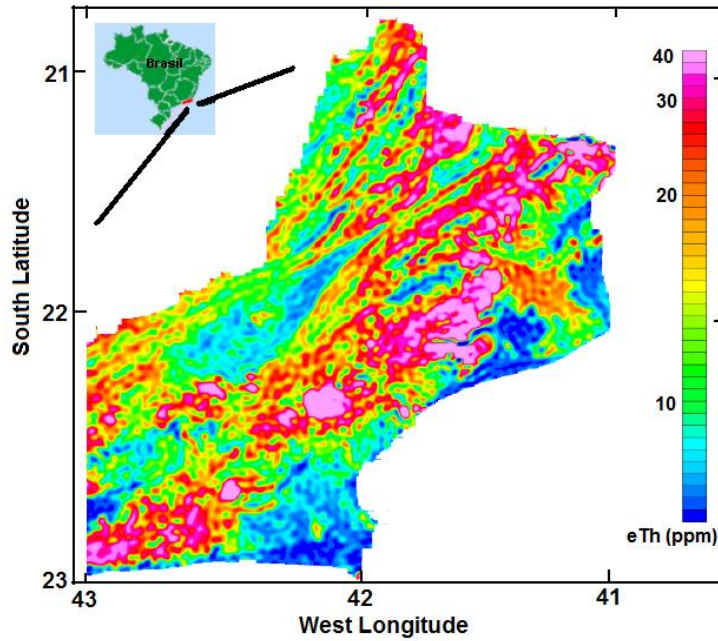


Figure 3a: Regional distribution of eTh in the eastern part of the state of Rio de Janeiro (Brazil) derived from results of airborne radiometric surveys.

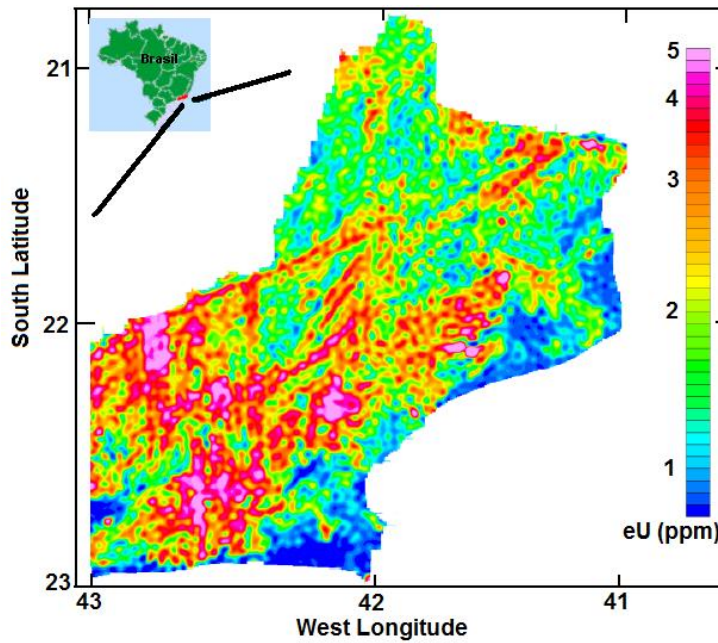


Figure 3b: Regional distribution of eU in the eastern part of the state of Rio de Janeiro (Brazil) derived from results of airborne radiometric surveys.

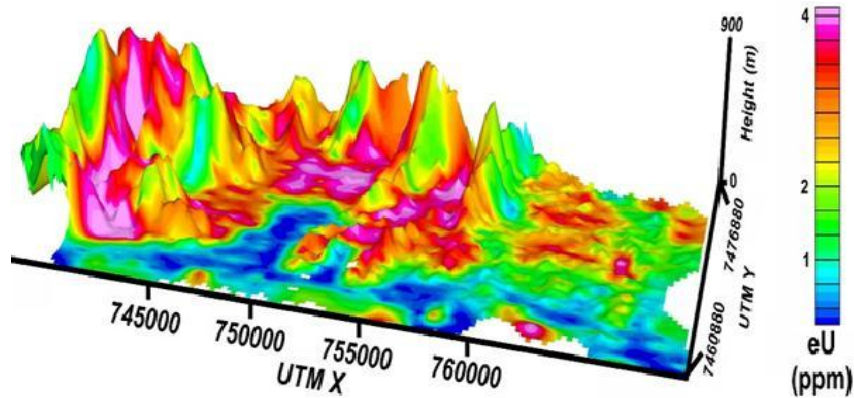


Figure 4: Distribution of eU draped on model representation of topography in the study area.

Similar trends can also be seen in the regional distributions of eTh and potassium illustrated in Figure 5. The abundance values of eTh are greater than 10 ppm in areas of high elevation in the northwestern parts, while belts of relatively low concentrations (less than 5 ppm) occur in the low-lying southern parts. In the case of potassium relatively high values ( $> 1\%$ ) occur in the northwestern parts while belts of relatively low concentrations ( $< 1\%$ ) occur in the southern parts. We conclude that topography plays a significant role in the regional distribution of radioelements in the study area.

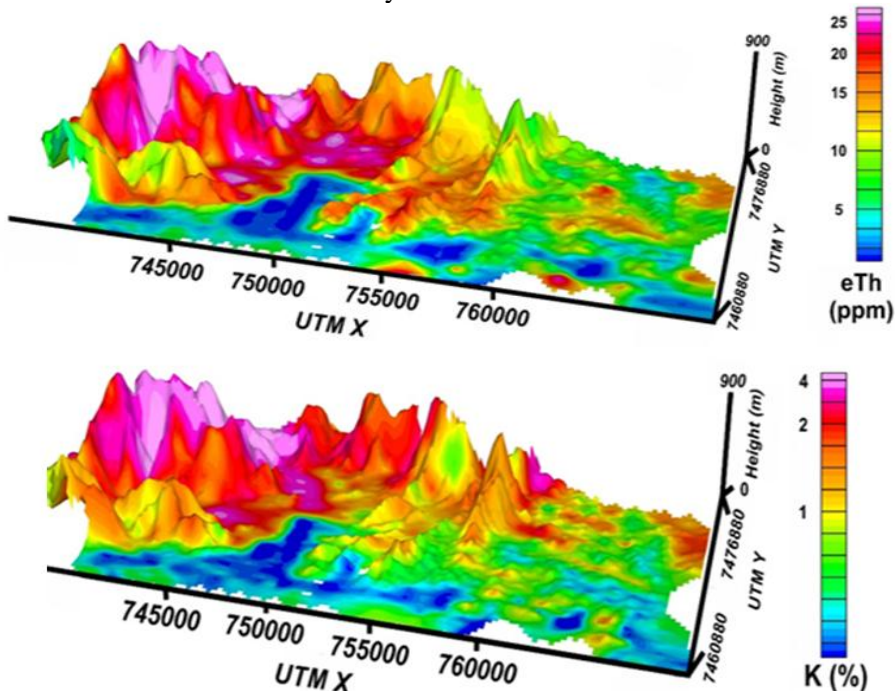


Figure 5: Distributions of eTh (upper panel) and potassium (lower panel), draped on model representations of topography in the study area.

### 3.2 Ground Surveys

Ground surveys included measurements of abundances of radioactive elements in soils at twelve localities in the municipality of Saquarema, in the state of Rio de Janeiro. Three different experimental techniques were employed: scintillation detector, solid-state detector and instrumental neutron activation analysis. Use of portable scintillation detectors (of the type NaI - Tl activated) allows rapid in-situ measurements of naturally radioactive elements. However, energy resolutions of such detectors for identifying the gamma radiations are poor. On the other hand high purity germanium detectors (HPGe) have much better energy resolution, allowing identification of several low-energy (< 1 Mev) gamma emissions by the elements in the radioactive series. Neutron activation analysis allows simultaneous measurement of several major and minor elements, but for obvious reasons the instrumental setup is not portable.

The locations of the sample sites are indicated in the map of Figure 6. Also indicated in this map are the main soil types and other local features such as rivers and islands as well as saline water bodies and urban areas. According to the classification system of [27] Ultisol, characterized by its high clay activity, is the predominant type of soil in the study area. Other soil types present in the area include Spodosol, Gleysol, Entisol and Organosol. Samples 1 to 9 are predominantly Entisol, while 10 and 12 are Ultisol.

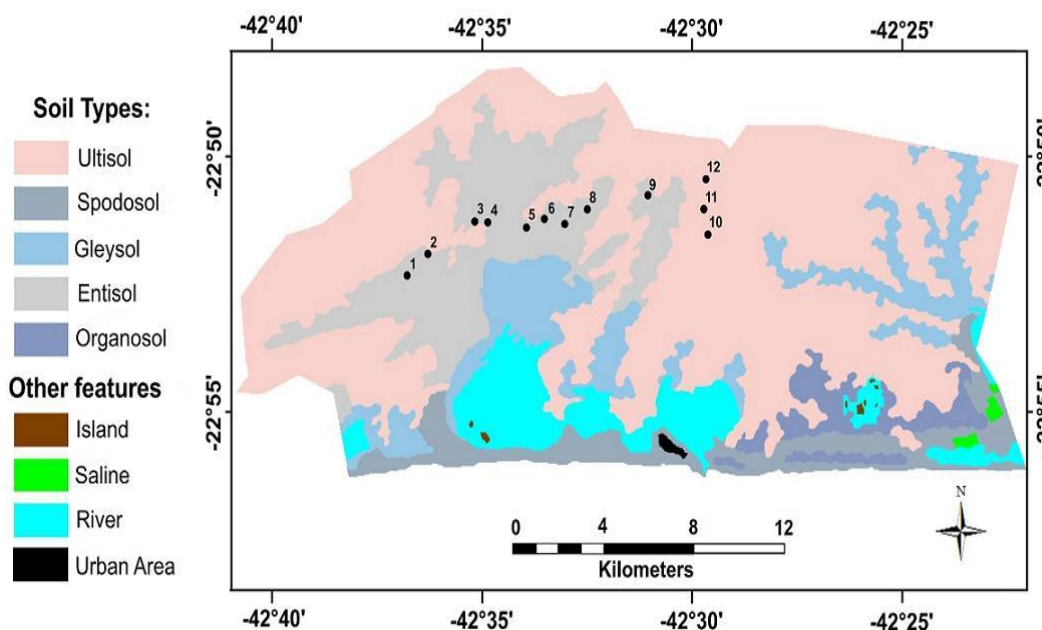


Figure 6: Map of soil cover in Saquarema municipality, in the coastal area of Rio de Janeiro. The numbers refer to locations of soil samples.

#### 3.2.1 Measurements using scintillation detector

The scintillation detector used in ground gamma-ray spectrometry survey is an Exploranium GR-320 portable device. The main components of this equipment include a sodium iodide (NaI) thallium activated crystal and an associated electronic system that allows automatically maintaining the position of energy channels with respect to peaks of U (ppm), Th (ppm) and K (%). The calibration tests were carried out at the facilities available

at the Institute of Radiation Detection (IRD) in Rio de Janeiro [28]. These include 18 concrete calibration pads with concentrations of uranium, thorium and potassium comparable to those found in normal geologic media. The procedure adopted for field measurements is in accordance with the recommendations outlined in [29]. Initially the detector was kept in contact with the ground during the measurement period. A second set of measurements were made by placing the detector at a height of approximately one meter above the ground level. In this case, the instrument detects gamma rays from a circular area of approximately 10m radius. The sampling time for measurements was set to a value of 100s. Details of the methodology employed in use of the portable spectrometer and its calibration are described in detail by [30, 31].

Two sets of samples were collected: the first one at shallow depths of up to 20 cm and a second set from depths of 20 to 40 cm. According to the results obtained mean values of uranium, thorium and potassium in soils are respectively  $3.5 \pm 1.0$  ppm,  $18.4 \pm 3.6$  ppm and  $1.5 \pm 0.3$  %. The mean values of uranium and thorium are higher than those found for soil samples in the interior parts of Brazil [32]. The ratios U/K and Th/K are found to have mean values of 4.9 and 22.8, which are again higher than the corresponding values for soil samples elsewhere. Table 1 provides a summary of the results obtained.

Table 1: Results of measurements on soil samples at twelve sites, using portable scintillation detector. Sample locations are indicated in Universal Transverse Mercator system (UTM). Symbol  $\sigma$  refers to standard deviation.

Sample ID	Soil Type	Coordinates		U (ppm)		Th (ppm)		K (%)	
		UTM X	UTM Y	Mean	$\sigma$	Mean	$\sigma$	Mean	$\sigma$
1	Entisol	744910	7468638	4.7	0.8	23.8	10.9	2.4	0.3
2		745747	7469408	2.6	0.9	16.1	2.4	0.3	0.1
3		747710	7470546	2.2	1.3	19.6	5.1	1.1	0.2
4		748239	7470546	3.2	0.4	16.6	2.8	-----	-----
5		749804	7470285	4.1	0.8	22.8	2.8	2.2	0.2
6		750527	7470571	3.5	1.3	16.6	2.8	1.1	0.2
7		752278	7470882	3.2	0.6	18.4	1.1	0.7	0.1
8		751362	7470384	4.4	1.8	22.4	2.1	3.1	0.3
9		754747	7471378	2.9	1.3	20.3	5.8	-----	-----
10	Ultisol	757162	7469894	4.9	1.4	16.2	2.9	-----	-----
11		757035	7470808	3.2	0.9	13.7	1.8	-----	-----
12		757122	7471885	3.1	0.5	13.8	2.1	1.1	0.1
Mean				3.5	1.0	18.4	3.6	1.5	0.3

### 3.2.2 Measurements using solid-state detector

The methodology employed in the use of solid state high-purity germanium (HPGe) detector has been described in the literature [33, 34]. The detector used in the present work has a diameter of 56 mm, length of 38.5 mm and has relative efficiency of 20% and resolution of 1.8 keV (kilo electron-volts) at 1330 keV and 0.7 keV at 22 keV. Use of HPGe detector allows determination of uranium based on intensity of the 63.3 keV photo peak emitted by  $^{234}\text{Th}$ , corrected for the interfering effect of the 63.9 keV photo peak of  $^{232}\text{Th}$  (the contribution of  $^{231}\text{Th}$  is relatively small and can be neglected for purposes of the



present work). The correction for contribution of <sup>232</sup>Th is based on the activity ratio of <sup>228</sup>Ac relative to <sup>232</sup>Th [33]. The relation used for determining intensity (C) values is:

$$C\left({}^{234}\text{Th}, 63.3\right) = C(63) - \frac{\varepsilon(63.9) * I\left({}^{232}\text{Th}, 63.9\right)}{\varepsilon(63.9) * I\left({}^{228}\text{Ac}, 338.32\right)} C\left({}^{228}\text{Ac}, 338.32\right) \quad (1)$$

where  $\varepsilon(E)$  is the total peak efficiency,  $I(E)$  is the emission probability and  $m$  the mass. Samples collected for measurements using solid state HPGe detector are from the same localities as those indicated in Figure 5. The procedures used in measurements by HPGe are similar to those discussed in the literature [35, 36]. According to the results obtained mean values of uranium and thorium in soils are respectively  $4.3 \pm 1.3$  ppm and  $19.4 \pm 1.6$  ppm. The mean values of uranium and thorium are in reasonably good agreement with those obtained using scintillation detector. Table 2 provides a summary of the results obtained.

Table 2: Results of measurements on soil samples at twelve sites, using HPGe detector. See caption of Table 1 for details.

Sample ID	Soil Type	Coordinates		U (ppm)		Th (ppm)	
		UTM X	UTM Y	Mean	$\sigma$	Mean	$\sigma$
1	Entisol	744910	7468638	4.2	1.4	28.4	2.1
2		745747	7469408	0.9	0.6	10.9	1.1
3		747710	7470546	3.1	1.1	17.8	1.6
4		748239	7470546	2.4	0.9	19.0	1.5
5		749804	7470285	5.2	1.4	26.4	1.8
6		750527	7470571	5.3	1.4	19.3	1.5
7		752278	7470882	3.8	1.2	22.3	1.7
8		751362	7470384	4.6	1.4	19.9	1.8
9		754747	7471378	3.2	1.1	22.7	1.7
10	Ultisol	757162	7469894	4.7	1.3	15.4	1.4
11		757035	7470808	9.6	2.3	22.4	1.8
12		757122	7471885	5.1	1.4	9.4	1.2
Mean				4.3	1.3	19.4	1.6

### 3.2.3 Instrumental neutron activation analysis (INAA)

The methodology for neutron activation analysis, described in detail by [37, 38], were adopted in the present work. Identical sets of samples were also collected for measurements using instrumental neutron activation analysis. According to the results obtained mean value of uranium in soils is  $3.8 \pm 0.3$  ppm while that for thorium is  $17.3 \pm 0.8$  ppm. The differences in the mean values of uranium and thorium are not significant, when compared with the uncertainties of other methods. Table 3 provides a summary of the results obtained.

Table 3: Results of measurements of U and Th in soil samples at twelve sites, by neutron activation analysis (INAA).

Sample ID	Soil Type	Coordinates		U (ppm)		Th (ppm)	
		UTM X	UTM Y	Mean	$\sigma$	Mean	$\sigma$
1	Entisol	744910	7468638	4.4	0.4	26.5	1.6
2		745747	7469408	2.2	0.2	9.6	0.4
3		747710	7470546	1.9	0.1	11.7	0.5
4		748239	7470546	4.2	0.4	23.9	0.8
5		749804	7470285	3.6	0.3	23.2	0.8
6		750527	7470571	3.9	0.2	22.5	0.8
7		752278	7470882	4.8	0.4	15.2	0.8
8		751362	7470384	3.8	0.1	16.6	0.8
9		754747	7471378	2.3	0.2	18.6	0.8
10	Ultisol	757162	7469894	4.1	0.3	10.7	0.5
11		757035	7470808	6.4	0.5	19.2	0.8
12		757122	7471885	3.3	0.2	9.4	0.4
Mean				3.8	0.3	17.3	0.8

### 3.2.4 Comparative analysis

A comparative analysis of the results of gamma spectrometry carried out using portable scintillation (GR-320) and solid state (HPGe) detectors as well as those obtained by instrumental neutron activation analyses (INAA) are illustrated in the upper panel of Figure 7 for uranium and lower panel of the same figure for thorium.

Note that there is reasonable agreement between the results by the three methods. For example, the mean values for uranium obtained by the three methods are 3.5, 4.3 and 3.7 ppm respectively. The differences between the means are not statistically significant. In the case of thorium the mean values obtained for the three methods are 18.4, 19.4 and 22.7 ppm respectively. In this case, the results indicate that the agreement is better between results obtained by portable and solid state detectors. Similar results were also obtained in measurements of potassium abundances.

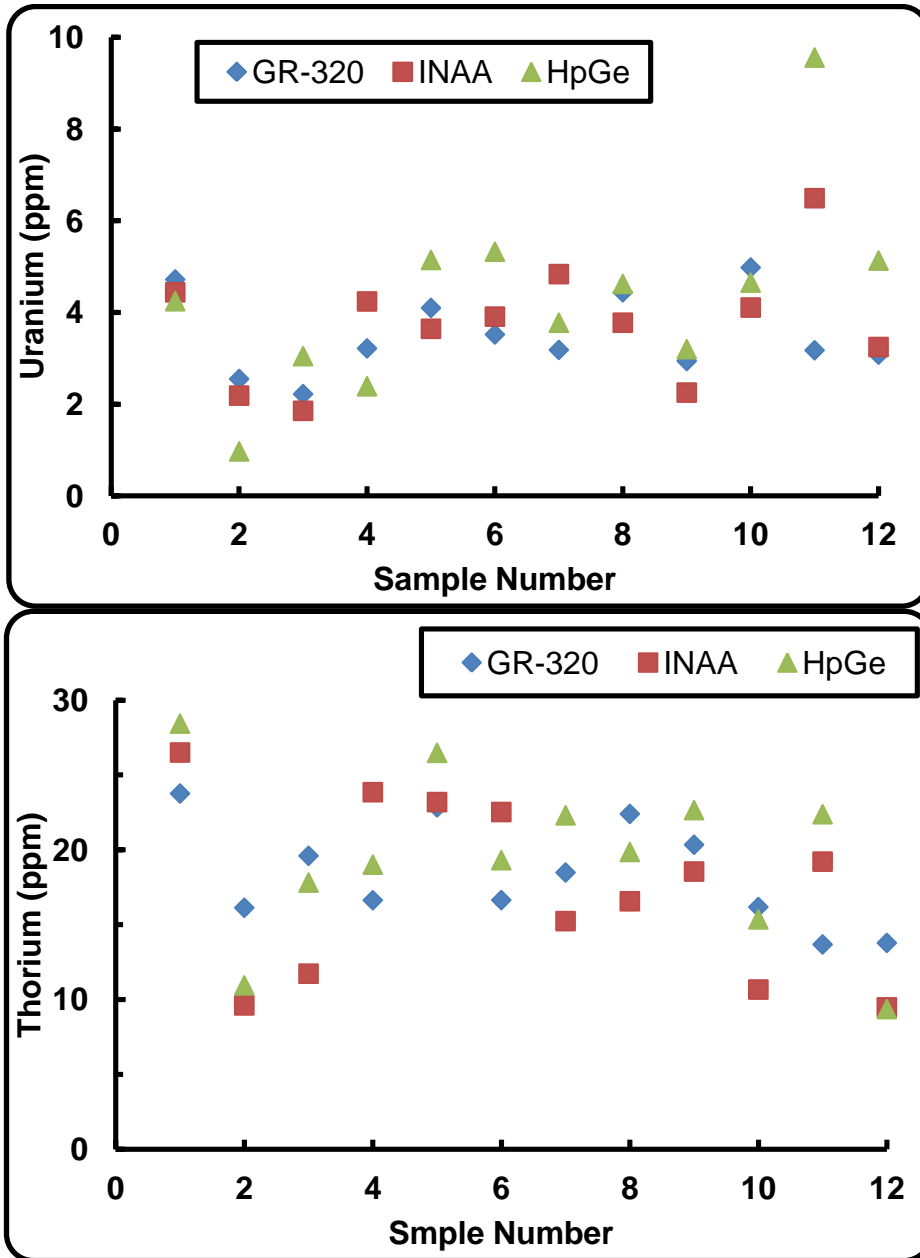


Figure 7: Comparison of the abundances of uranium (upper panel) and thorium (lower panel) in soils at 12 sites in the study area, determined by portable spectrometer GR-320 (lozenges), solid state detector (triangles) and INAA (squares).

#### 4 Mobility of Radionuclides

The mobility patterns of radionuclides in the Saquarema region is greatly influenced by weathering and hydrological processes occurring in the southeastern flank of the Serra do Mar escarpment. The area is characterized by a series of multiple southeast trending valleys

and ridges. Results of airborne surveys reported in the present work (see Figures 3 and 4) have mapped the radioelement distributions along closely spaced flight lines, following roughly the valley and ridge system. Results of ground surveys (discussed in section 3 of the present work) have been helpful in determining abundances in soil samples. The map of Figure 8 illustrates the topographic variations of the area selected for ground surveys. Also indicated in this map are the flight lines of airborne surveys, as well as locations of ground surveys. Many valleys are characterized by high drainage density and are known to transport natural radionuclides. Hence the results of ground surveys should be considered as indicative of cumulative end products of mobile processes driven by weathering and fluvial transport.

The regional distributions of uranium, thorium and potassium, illustrated in Figures 4 and 5 reveal that areas of high elevations in the northwestern border of the study area (adjacent to the Serra do Mar continental escarpment) are characterized higher concentrations of radionuclides relative to those in the low-lying plains. We consider the systematic decrease in the abundances of radioactive elements with distance from areas of elevated topography as consequence of weathering and erosion. In the present work, our interest is in examining not only the general trends in mobility of the natural radionuclides but also characteristics of their relative movements within the study area.

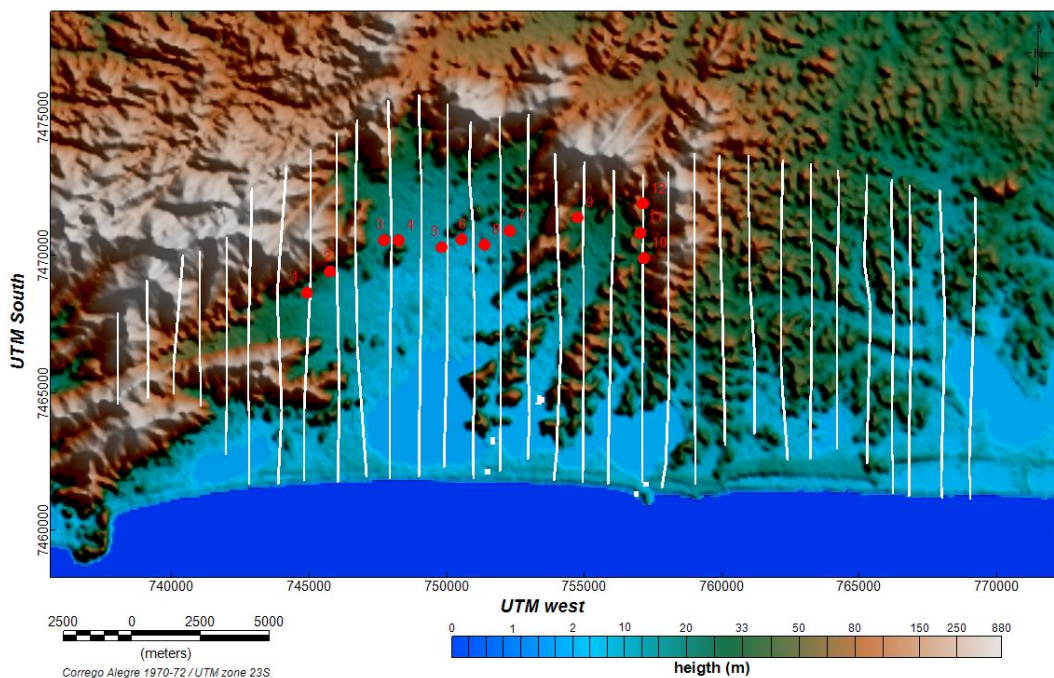


Figure 8: Topographic variations of the area selected for ground surveys. The lines indicate flight paths of airborne surveys and the red circular symbols indicate sites of ground surveys.

#### 4.1 Indications of Relative Movements

Some insights into the general trends in the relative mobility can be obtained by considering the geographic distributions of the ratios of radionuclides. Consider for

example the distribution of Th/K and U/K ratios illustrated in the map of Figure 9. Note that high values of Th/K are found in areas with altitudes of less than 10 meters, while regions with altitudes higher than 100 meters are characterized by relatively low values. A similar trend can also be seen in the distribution of U/K (lower panel of Figure 9).

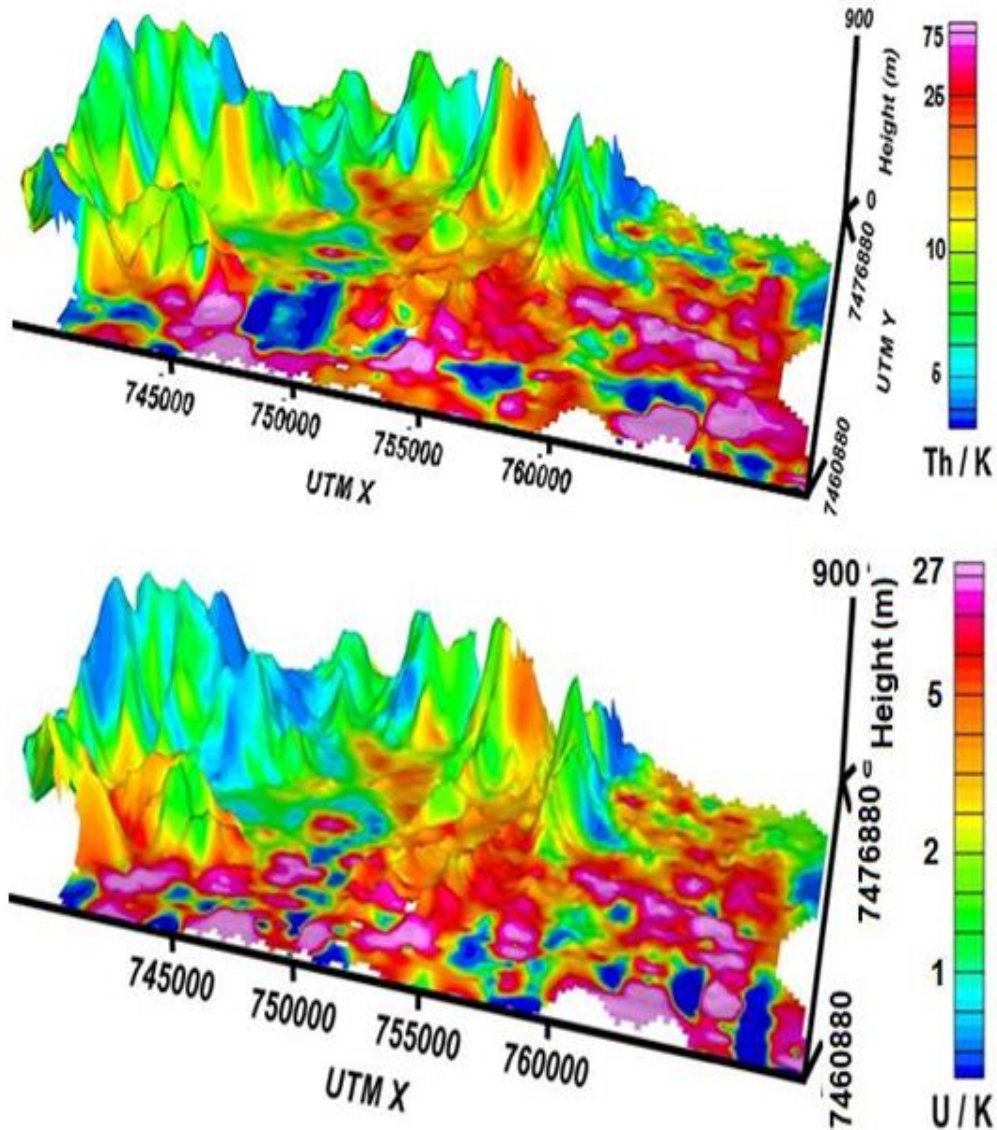


Figure 9: Regional distributions of the ratios Th/K (upper panel) and U/K (lower panel) in the Squarema region, draped over model representations of topography.

Since potassium is usually associated with the clay fractions, the observed trends of decrease in Th/K ratio are indications of steady enrichment of thorium along the migration paths. We conclude that weathering processes have led to gradual removal of potassium-rich clay fractions along the path from high altitudes to flat-lands. Thus, even though the absolute values of the abundances of thorium decrease with distance from the source region the relative enrichment process with respect to potassium prevails and seems

to be a characteristic feature of the weathering process. Such trends are contrary to those of the absolute abundances, illustrated in Figures 4 and 5.

As in the case of Th/K, high values of U/K are found in areas with altitudes of less than 10 meters, while regions with altitudes higher than 100 meters are characterized by relatively low values. It is indication that weathering processes have led to gradual removal of potassium-rich clay fractions along the migration path. Consequently, there has been relative enrichment of uranium with respect to potassium along the path from mountainous areas to flat lands. Again, this is contrary to the trend of absolute abundances, illustrated in Figures 4 and 5.

The distribution of U/Th, illustrated in Figure 10, reveals that U/Th values in the range of 0.2 to 1.0 in areas with altitudes of less than 10 meters, while regions with altitudes higher than 100 meters are characterized by relatively low values of less than 0.1. Such features are indications of enrichment of uranium relative to thorium in the study area. The enrichment process is believed to be related to the higher mobility of elements in the radioactive series of uranium. It may also be considered as a consequence of gradual retention of thorium-rich materials associated with heavy mineral fractions during its movements through soil layers.

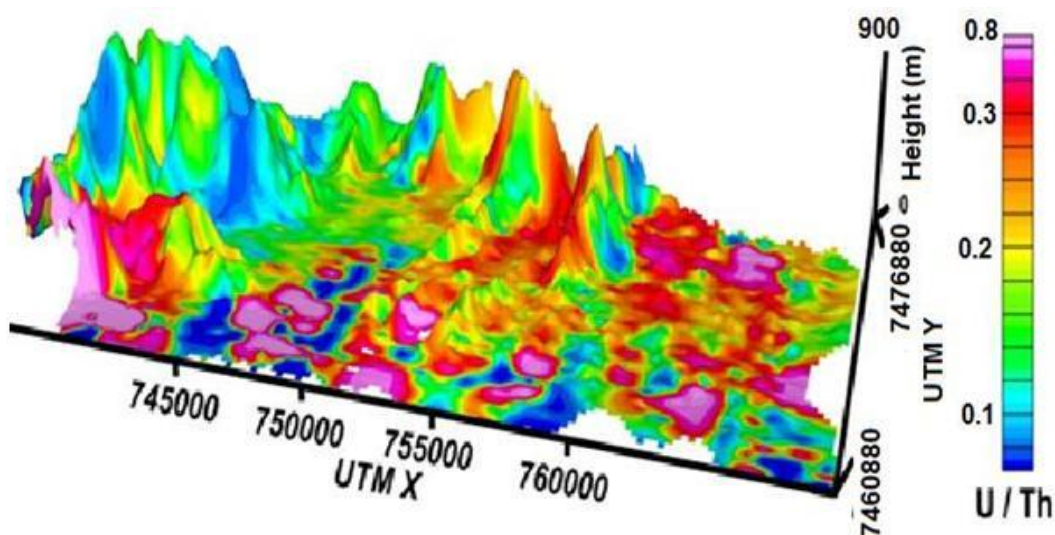


Figure 10: Regional distribution of U/Th ratios, draped over model representation of topography in the study area.

#### 4.2 Fits to Diffusion Models

The geographic distribution patterns in the maps of Figures 4 and 5 are clear indications that radioactive elements have migrated from the source region (the Serra do Mar escarpment) downstream into the sediment covered plains of the coastal area. The objective here is to model this migration as the result of an equivalent of a particle diffusion process in the geologic environment of the study area.

We assume that particle transport can be mathematically described as simple, one-dimensional diffusion equation [39]:

$$\frac{\partial C}{\partial t} = D \frac{\partial^2 C}{\partial x^2} \tag{2}$$

where  $C$  is the particle concentration,  $t$  is time,  $D$  the particle diffusion coefficient and  $x$  the distance downslope. One particular solution to equation 2 is:

$$C(x, t) = C_0 + \frac{M}{2\sqrt{\pi D t}} \exp \left[ -\frac{x^2}{4 D t} \right] \tag{3}$$

where  $C_0$  is the background concentration in the source region (mg/kg) and  $M$  is a constant related to the tracer mass in the study area. Note that equation 3 is similar in form to a Gaussian:

$$\frac{C(x, t) - C_0}{(C_m - C_0)} = \frac{1}{\sigma \sqrt{2 \pi}} \exp \left[ -\frac{(x - \mu)^2}{2 \sigma^2} \right] \tag{4}$$

where  $C_m$  is a constant related to the maximum concentration of the element at the center of the study area,  $\mu$  is the downslope position of the maximum concentration and is the distance of transport of the entire center of mass of the study area, and  $\sigma$  is the spread of the peak and represents the transport distance caused by particle diffusion. In this study  $\sigma$  was determined by fitting a Gaussian of the form of equation 4 to the concentration-distance data. If the duration of transport episode is used as time even though it may not be continuous in time, a crude estimate of the particle diffusion coefficient can be obtained by noting that  $D = \sigma^2 / 2t$ .

In carrying out model fits we used results of experimental data obtained in the present work for 12 sites in the Saquarema region and also results for the source region reported by [21]. The distances of sample to source regions were estimated from information available in local geologic maps and results of regional gamma surveys. The parameter values employed in model fits are given in Table 4.

Table 4: Values of parameters employed in model fits.

Parameter	Uranium	Thorium
Background Concentration ( $C_0$ )	0	0
Maximum concentration ( $C_m$ )	9.5	50
Transport distance caused by particle diffusion ( $\sigma$ )	5000	5000
Downslope position of $C_m$ ( $\mu$ )	10 - 20	10 - 20

The results of fits of diffusion model (continuous curves) to observational data are illustrated in Figure 11 for Uranium (upper panel) and for Thorium (lower panel). The relatively good fit of observational data to model curves is indication that diffusion leads to depletion of radioactive elements along the migration path, starting from the high altitude source region and ending in the flat-lying low lands. This depletion process determines the systematic trend of decreasing abundances of all three radio-elements, in spite of the relative enrichment of thorium and uranium relative to potassium.

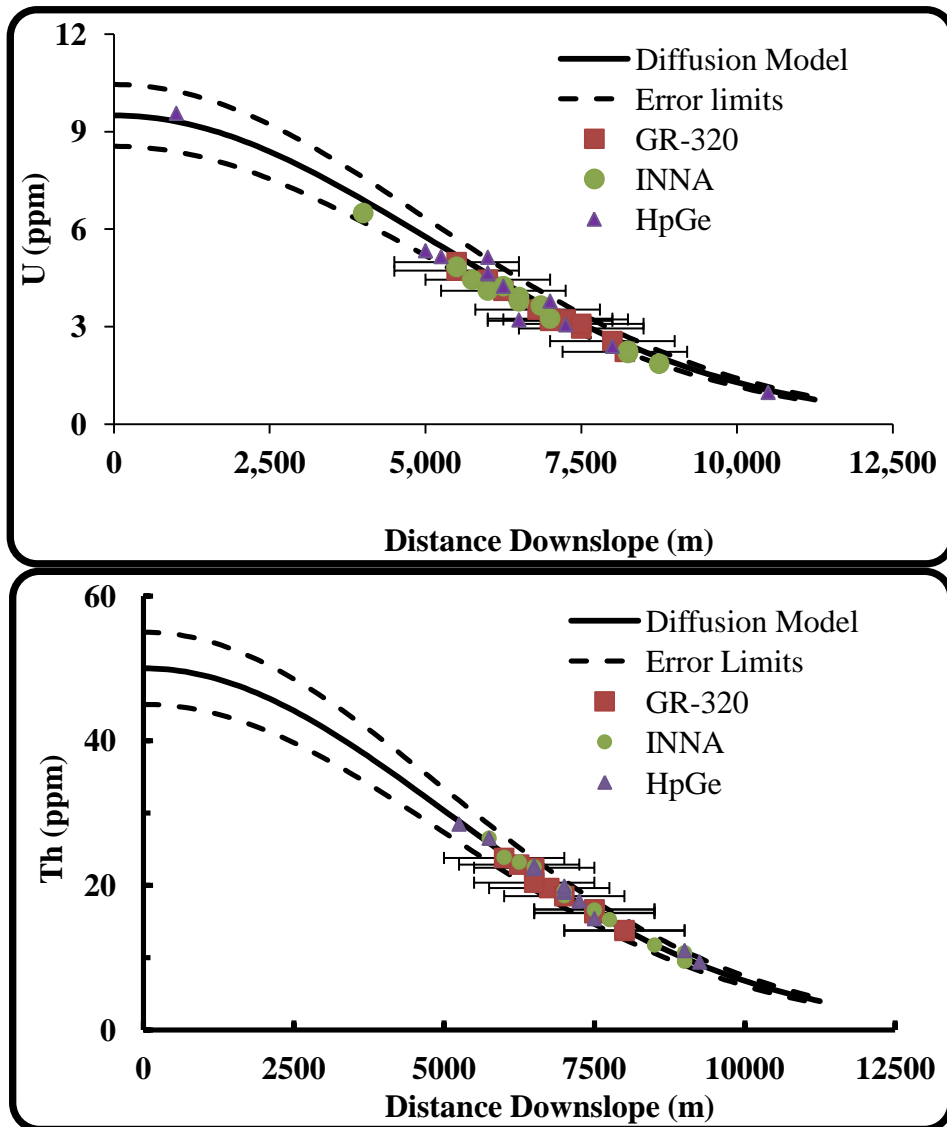


Figure 11: Fits of diffusion model (continuous curve) to observational data for uranium (upper panel) and for Thorium (lower panel). The dashed curves indicate error limits in model fits.

## 5 Distributions of Rare Earth Elements

The general aspects of geochemical differentiation of rare earth elements in the Earth and in the sedimentary cycle have been discussed [40, 41]. The chemical behavior of rare earth elements is governed by the systematic contraction of trivalent ionic radii with atomic number as the shielded electrons are added to the inner 4f shell and some of the elements, especially Ce and Eu occur in oxidation states other than +3, the main oxidation state of the group. Rare earth element geochemistry is commonly assessed using REE profiles, in which raw concentration data are normalized to standardized abundances for chondritic



meteorites, considered representative of the bulk Earth composition. This produces smooth patterns by suppressing differences in absolute abundances, and such profiles have distinctive shapes that may be indicative of compositional groupings or processes.

### 5.1 REEs in Soil Samples

In the present work we have measured REEs from the soil samples using neutron activation methods. Sample preparation can be a major problem with REE analysis as the bulk of these elements, particularly the heavier REEs (Dy-Lu), commonly resides in refractory accessory minerals such as zircon, sphene and garnet. REE data obtained was calibrated against results for certified and standard reference materials. The precision of this method is better than 5% with comparable accuracy. A summary of the results obtained is provided in Table 5 for twelve rare earth elements. In all soil samples the abundances of the first four of the lighter REEs (La, Ce, Pr and Nd) are relatively higher (in the range of 40 to 300ppm), compared with those (in the range of 5 to 10 ppm) of the remaining heavier REEs (Sm, Eu, Gd, Tb, Dy, Ho, Er, Tm, Yb and Lu).

Table 5: Rare earth element abundances (in ppm) of soil samples in Saquarema region, determined by instrumental neutron activation analysis (INAA).

ID	La	Ce	Nd	Sm	Eu	Tb	Dy	Ho	Er	Tm	Yb	Lu
1	107	215	94	15	1.4	1.5	1.9	2.2	2.6	2.9	3.3	0.7
2	37.0	78	33	6.5	1.3	0.9	1.1	1.3	1.5	1.7	1.9	0.4
3	51.2	107	43	8.4	1.4	0.4	0.5	0.6	0.7	0.8	0.9	0.2
4	86.0	176	65	11.7	0.8	1.3	1.6	1.8	2.1	2.3	2.6	0.5
5	95.0	194	79	14.7	1.6	1.7	2.6	3.4	4.2	4.9	5.8	0.8
6	92.0	192	78	15	1.3	1.8	2.4	2.9	3.5	4.1	4.6	0.6
7	65.2	133	55	10.3	1.4	1.2	1.9	2.6	3.3	4.0	4.7	0.6
8	64.5	133	53	9.7	1.0	1.1	1.5	1.9	2.3	2.7	3.1	0.5
9	83.0	168	69	12.7	1.3	1.1	1.5	1.9	2.4	2.8	3.2	0.4
10	44.3	93	37	8.1	0.9	1.5	2.9	4.3	5.7	7.1	8.5	1.3
11	85.0	177	75	14.5	1.9	2.3	3.6	4.8	6.1	7.3	8.6	1.2
12	44.7	90	37	7.7	1.6	0.9	1.4	1.8	2.2	2.6	3.0	0.4
<b>Mean</b>	71.2	146	59.8	11.2	1.3	1.3	1.9	2.5	3.0	3.6	4.2	0.6
<b>SD</b>	23.2	46.7	19.8	3.2	0.3	0.5	0.8	1.2	1.6	2.0	2.4	0.3

The relative pattern of abundances observed in samples of the present work is similar to those encountered in soil samples of other regions [42 – 44]. Another common characteristic refers to the differences relative to the abundances reported for chondrites [45, 46]. The abundance values of soil samples of the present study are, in general, 1~2 orders of magnitude higher than those of the chondrites. The variation of abundances in soil samples and the chondrite normalized patterns are illustrated in Figure 12. It reveals enrichment of light REEs relative to heavy REEs as well as the well known drop in abundance of Eu relative to other REEs. The negative Europium (Eu) anomaly noticed in soil samples appear to be controlled by the presence of feldspars in clay fractions. Thus the removal of feldspar during weathering and erosion will give rise to a negative Eu anomaly in the soil. Ce anomaly is not so much evident.

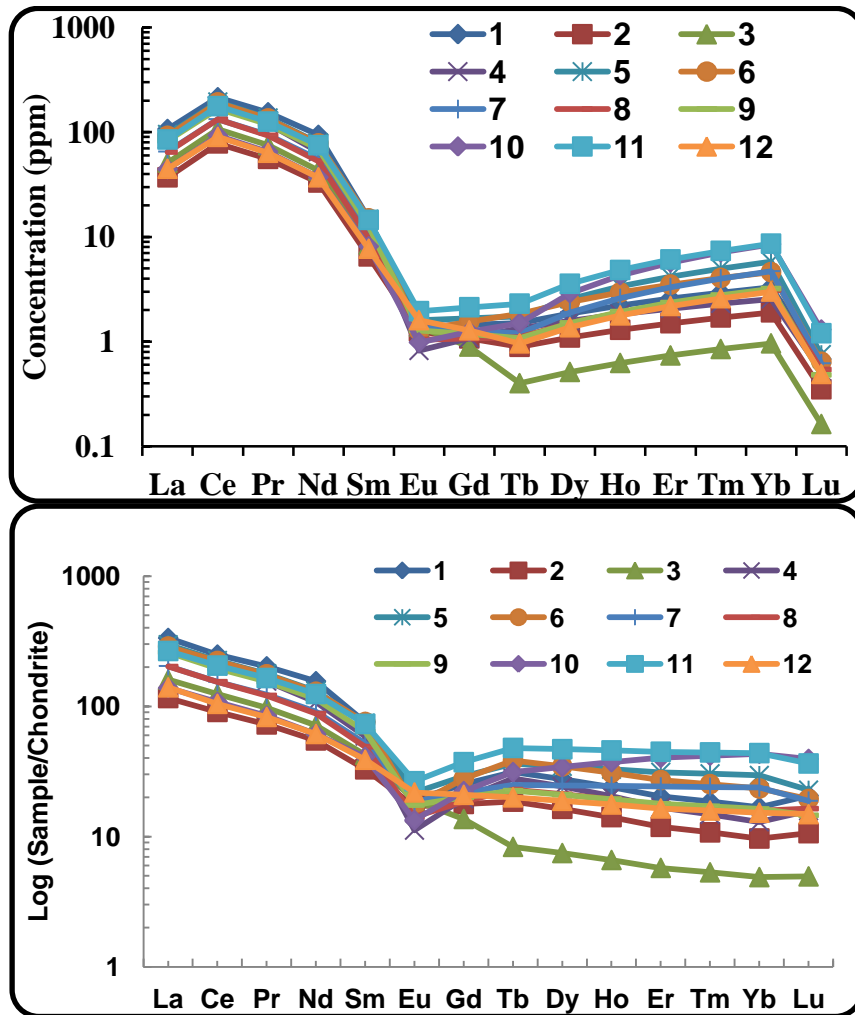


Figure 12: Abundances of REEs in soil samples (upper panel) and scaling with respect to chondrites (lower panel). The numbers refer to locations of samples.

## 5.2 Comparison with REEs in Basement Rocks and Beach Sands

The abundances of REEs discussed in section (4.1) refer to soil samples from locations which occupy intermediate positions along the migration paths of radioactive and rare earth elements. However, understanding its relative importance for the problem of mobility of REEs require comparison with corresponding values of the basement rocks as well as those of the beach sands of the coastal area. We consider in this context, REE abundances reported for Buena region monazites [14], Vermelha Beach sands [9, 10] in the state of Rio de Janeiro and Guarapari Beach sands in the state of Espirito Santo (ES), for the basement rocks of the state of Rio de Janeiro [21]. In comparing these results with the data for soil samples of the Saquarema region it is convenient to make use of values normalized to those of the chondrites. In the present work we make use of the relevant data for chondrites, reported by [46]. Such a comparison, illustrated in Figure 13, reveals that beach sands and monazites (curves A, B, C and D) are enriched by factors of  $10^3$  to  $10^5$  in REEs, relative to

those of chondrites. The enrichment is relatively high in light REEs (La, Ce, Pr and Sm) when compared with those of heavier REEs (Gd, Tb, Dy, Ho, Er, Tm, Yb and Lu).

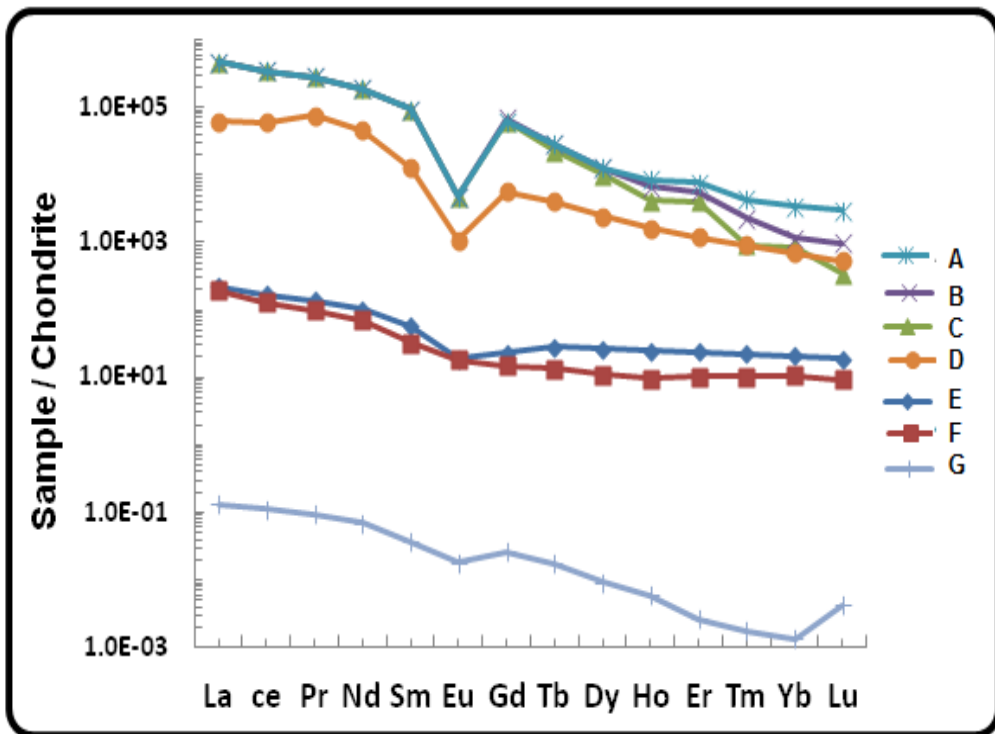


Figure 13: Concentrations of REE relative to chondrites in source rocks, soil samples and beach sands of the study area. (A) Buena region Monazite [14], (B) Vermelha Beach sand [9], (C) Guarapari sand [10], (D) Buena region Monazite [8], (E) Saquarema soil (this work), (F) basement rocks [18] and (G) Buena region groundwater [8].

Referring to Figure 13 note that the enrichment relative to chondrites is much less in basement rocks (curve F) and soils (curve E). As expected, abundances of REEs in groundwaters (curve G) are at least one or two orders of magnitude lower than those for soils and basement rocks. It must be pointed out here that this enrichment process is distinctly different from the relative enrichment of uranium and thorium with respect to potassium in soils, discussed earlier (see section 3.1). Another notable feature in Figure 13 is the presence of negative europium anomaly in beach sands and monazites (curves A, B, C and D) and its subdued presence in soils (curve E) and groundwater (G). It is almost absent in basement rocks (curve F).

## 6 Formation of Ore-grade Deposits

We now consider the implications of this enrichment process in the formation of ore-grade deposits of monazites. It seems reasonable to argue that removal of light fractions from mineral aggregates lead to reduction in mobility of accessory minerals. Obviously, mobility of monazites will be significant only as long as the lighter clay fractions remain attached to the mineral aggregates. Near total removal of lighter clay fractions leads to aggregates that

contain only the heavier accessory minerals, which remain as relatively immobile residue of the weathering process. Continued action of erosion brings in additional residues into this zone, which contributes to enrichment of accessory minerals and eventual formation of ore grade deposits of monazites in the coastal region.

It is possible to obtain approximate estimates of the time and distance scales of the ore-forming environment, from an analysis of the characteristics of the enrichment process illustrated in Figures 9 and 10 and the diffusion process illustrated in Figure 11. Variations in the values of Th/K ratios as a function of distance from the source region may be used for this purpose. The results obtained are illustrated in Figure 14 for the Guarapari and Saquarema regions. Note that a limiting value of  $10^9$  for the Th/K ratio has been adopted, which is in accordance with the results of Figure 13 for the monazites in the region of Guarapari (ES). This has also been adopted as the limiting value of Th/K ratio for the Saquarema region.

The source area of radioactive elements and REEs in the Guarapari region is about 65 km from the coast line, where Th/K ratio reaches value of  $10^9$ . In the Saquarema region the coast line is only 35 km from the source area of radioactive elements and REEs. However, Th/K ratio is postulated to reach its value for ore-grade deposits at a distance of approximately 45 km. The inevitable conclusion is that the ore-grade deposits of monazites in Saquarema region are located in the submerged part of the continental shelf, at a distance of about 10 to 20 km from the present coastline.

The time and distance scales associated with this enrichment process have been estimated based on the regional distribution of Th/K ratios. The results obtained indicate that submerged monazite deposits may be present along the offshore sand banks, in the coastal region of the state of Rio de Janeiro. The geographic association between the source region and Monazite deposits is illustrated in Figure 15 for Guarapari (upper panel) and Saquarema (lower panel) regions. It is possible that the formation of monazite deposits in continental shelf areas took place during periods of low sea-level. These results may be useful in locating under-water monazite deposits in other parts of continental shelf with similar geologic context.

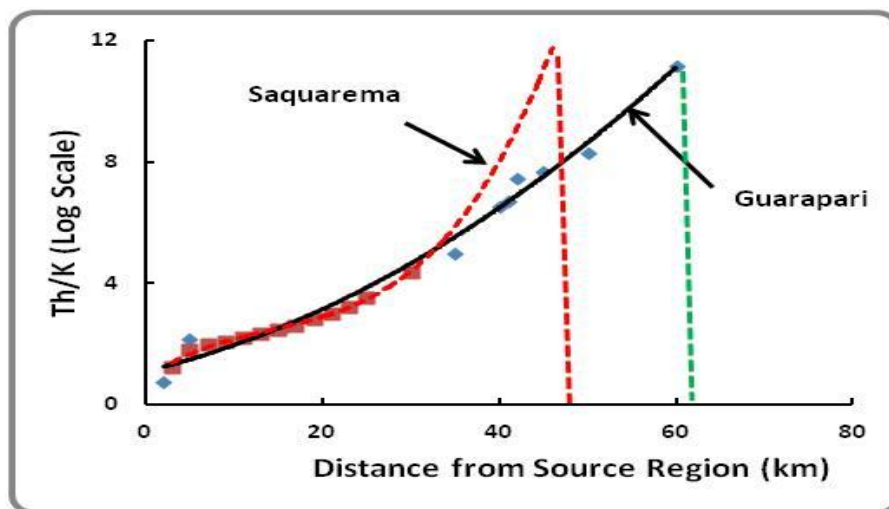


Figure 14: Variation of Th/K ratio with distance from the source regions of Saquarema and Guarapari. The dashed curves are polynomial fits to observational data. The vertical lines indicate domain limits.

## 7 Discussion and Conclusions

Analysis of ground and airborne radiometric data as well as rare earth element abundances in soils in the Saquarema region (State of Rio de Janeiro, Brazil) has allowed new insights into the mobility of mineral aggregates containing monazites, under tropical weathering conditions. The characteristics of the regional distributions of radioactive elements, as revealed in results of airborne radiometric surveys, indicate that topography and fluvial systems play dominant roles in determining the transportation of weathered material. The mobility pattern is characterized by a systematic depletion trend of radioactive elements along the migration paths, extending from regions of relatively high topography to the low-lying flatlands. Superimposed on the general depletion trend are indications of relative enrichment of uranium and thorium with respect to potassium along the migration paths. On the other hand, analysis of data on rare earth elements abundances in soils and beach sands point to the existence of a complementary process responsible for formation of ore-grade deposits of monazites along the coastal regions. There are indications that the enrichment process is related to transport processes occurring along the coast by long-shore currents. Beach formation leads to rapid removal of lighter clay fractions from the weathered material, which leaves behind a residue of heavier fractions rich in sands. This process gets enhanced in the presence of heavier REEs in the sand fraction. Note that this enrichment process in the coastal region is distinctly different from the depletion process operating in the interior regions away from the coastal region.



Figure 15: Locations of the source regions of monazites and ore-grade deposits in the Guarapari area (upper panel). An equivalent hypothesized scheme for monazites of the Saquarema region is shown in the lower panel.

**ACKNOWLEDGEMENTS:** We thank CPRM (Companhia Pesquisa de Recursos Minerais, Brazil) for providing data sets of airborne surveys used in this work. The first author has been recipient of a Ph.D. scholarship granted by CAPES, Brazil. We acknowledge help of Miss. Suze Guimarães (Observatório Nacional) in elaboration of maps with 3D perspectives.

## References

- [1] J.J.W. Rogers and A.S. Adams, Thorium, *Handbook of Geochemistry*, Ed. K.H. Wedepohl, Vol. II/5, Springer-Verlag, Berlin, (1969), 90-E.
- [2] J.J.W. Rogers and A.S. Adams, Uranium, *Handbook of Geochemistry*, Ed. K.H. Wedepohl, Vol. II/5, Springer-Verlag, Berlin, (1969), 92-E.
- [3] J. Wilford, A weathering intensity index for the Australian continent using airborne gamma-ray spectrometry and digital terrain analysis. *Geoderma*, **183/184**, (2012), 124-142.
- [4] J.A.S. Adams and C.E. Weaver, Thorium to uranium ratios as indications of sedimentary processes: example of concept of geochemical facies. *Am. Assoc. Pet. Geol. Bull.*, **42**, (1958), 387–430.
- [5] P. Henderson, *Rare Earth Element Geochemistry*, Elsevier Science Publishers B.V., Amsterdam, (1984).
- [6] R.M.R. Almeida, D.C. Lauria, A.C. Ferreira and O. Sracek, Groundwater radon, radium and uranium concentrations in Região dos Lagos, Rio de Janeiro State, Brazil. *J Environmental Radioactivity*, **73**, (2004), 323–334.
- [7] A.C. Freitas and A.S. Alencar, Gamma dose rates and distribution of natural radionuclides in sand beaches-Ilha Grande, Southeastern Brazil, *J. Environ. Radioactivity*, **75**, (2004), 211-223.
- [8] D.C. Lauria, R.M.R. Almeida and O. Sracek, Behavior of radium, thorium and uranium in groundwater near the Buena Lagoon in the coastal zone of the State of Rio de Janeiro, Brazil, *Environmental Geology*, **47**, (2004), 11–19.
- [9] A.S. Alencar and A.C. Freitas, Reference levels of natural radioactivity for the beach sands in a Brazilian southeastern coastal region, *Radiation Measurements*, **40**, (2005), 76-83.
- [10] R.M. Anjos, R. Veiga, K. Macario, C. Carvalho, N. Sanches, J. Bastos and P.R.S. Gomes, Radiometric analysis of Quaternary deposits from the southeastern Brazilian coast, *Marine Geology*, **229**, (2006), 29–43.
- [11] R.C.L. Figueira, M.G. Tessler, M.M. de Mahiques and I.I.L. Cunha, Distribution of  $^{137}\text{Cs}$ ,  $^{238}\text{Pu}$  and  $^{239} + ^{240}\text{Pu}$  in sediments of the southeastern Brazilian shelf-SW Atlantic margin, *Sci. Total Environment*, **357**, (2006), 146-59.
- [12] R.M. Anjos, R. Veiga, C. Carvalho, K. Macario and P.R.S. Gomes, Geological provenance of quaternary deposits from the southeastern Brazilian coast, *Nuclear Physics A*, **787**, (2007), 642c - 647c.
- [13] R. Veiga, N. Sanches, R.M. Anjos, K.J. Macario, J. Bastos, M. Iguatemy, J.G. Aguiar, A.M.A. Santos, B. Mosquera, C. Carvalho, M. Baptista Filho and N.K. Umisedo, Measurement of natural radioactivity in Brazilian beach sands, *Radiation Measurements*, **41**, (2006), 189–196.

- [14] J.M. Godoy, M.D.P. Godoya and C.C. Aronne, Application of Inductively Coupled Plasma Quadruple Mass Spectrometry for the determination of Monazite ages by Lead isotope ratios, *J. Braz. Chem. Soc.*, **18**, (2007), 969-975.
- [15] I.R. Santos, W.C. Burnett and J.M. Godoy, Radionuclides as tracers of coastal processes in Brazil: Review, synthesis, and perspectives, *Brazilian Journal of Oceanography*, **56**, (2008), 115-131.
- [16] R.M. Anjos, K.D. Macario, T.A. Lima, R.Veiga, C. Carvalho, P.J.F. Fernandes, M. Vezzone and J. Bastos, Correlations between radiometric analysis of Quaternary deposits and the chronology of prehistoric settlements from the southeastern Brazilian coast, *Journal of Environmental Radioactivity*, **101**, (2010), 75–81.
- [17] C. Carvalho, R.M. Anjos, R. Veiga and K. Macario, Application of radiometric analysis in the study of provenance and transport processes of Brazilian coastal sediments, *Journal of Environmental Radioactivity*, **102**, (2011), 185 - 192.
- [18] F.F.M de Almeida, Origem e Evolução da Plataforma Brasileira, *Boletim da Divisão de Geologia Mineral, DNPM, Rio de Janeiro*, **241**, (1967), 1-36.
- [19] F.F.M. de Almeida, Diferenciação Tectônica da Plataforma Brasileira In: *Proceedings of Congresso Brasileiro de Geologia, Salvador*, **23**, (1969), 29-46.
- [20] M. Heilbron, W. Mohriak, C.M. Valeriano, E. Milani, J.C.H. Almeida and M. Tupinambá, From Collisional to Extension: The Roots of The Southeastern Continental Margin of Brazil, In: Mohriak W.U. & Talwani M. (eds.) *Geology & Geophysics of Continental Margin*. AGU Geophysical Monograph, (2000), 1-32.
- [21] S.M. Viana, C.V. Valladares and B.P. Duarte, Geoquímica dos ortognaisses do Complexo Região dos Lagos, Araruama-Cabo Frio, Rio de Janeiro, Brasil. *Revista Brasileira de Geociências*, **38**, (2008), 488-500.
- [22] BARMP – Brazil Airborne Radiometric Mapping Project, *Technical Report and survey Atlas*, (1997), 18p.
- [23] B.R.S. Minty, Fundamentals of airborne gamma-ray spectrometry. *AGSO Journal of Australian Geology & Geophysics*, **17**, (1997), 39-50.
- [24] J.R. Wilford, P.N. Bierwirth and M.A. Craig, Application of airborne gamma-ray spectrometry in soil/regolith mapping and applied geomorphology, *Journal of Australian Geology & Geophysics*, **17**, (1997), 201-16.
- [25] B. Dickson, Interpretation of aerial gamma-ray – adding the geochemical factors. *Journal of Australian Geology & Geophysics*, **17**, (1997), 187-200.
- [26] B. Dickson, Recent advances in aerial gamma-ray surveying. *Journal of Environmental Radioactivity*, **76**, (2004), 225-236.
- [27] EMBRAPA (Empresa Brasileira de Pesquisa agropecuária) *The Brazilian Soil Classification System (In Portuguese)*, Centro Nacional de Pesquisa de Solos, Brasília, (1999), 412p.
- [28] P.M.C. Barreto, Radioactive concrete sources at IRD/CNEN, Brazil, for the calibration of uranium exploration and environment field instruments. *Report IRD/DEX-3/CNEN*, (1986), 66p.
- [29] IAEA - International Atomic Energy Agency, Guidelines for radioelement mapping using gamma ray spectrometry data. *Vienna, IAEA – TECDOC*, 1363, 92-0-108303-3, (2003).
- [30] C.C. Conti, Medida de Kerma no Ar e Determinação de Coeficientes de Conversão para a Devido à radiação Gama Ambiental, (1999), 191p. *Unpublished Ph.D. Thesis*, Universidade Federal do Rio de Janeiro.

- [31] J.J. Silva, F. Lamego and V.M. Hamza, A Comparative Study of Ground and Airborne Gamma Measurements in Saquarema (RJ): Implications for Determination of Radiogenic Heat of Basement Rocks beneath tropical soil cover, *Proceedings of the 12th International Congress of the Brazilian Geophysical Society*, August 15-18, (2011), Rio de Janeiro, Brazil.
- [32] S.N.P. Guimarães, V.M. Hamza and J.J. Silva, Airborne geophysical surveys in the north-central region of Goiás (Brazil), *Journal of Environmental Radioactivity*, **116**, (2013), 10 – 18.
- [33] C.A. Papachristodoulou, P.A. Assimakopoulos, N.E. Patronis and K.G. Ioannides, Use of HPGe gamma-ray spectrometry to assess the isotopic composition of uranium in soils, *Journal of Environmental Radioactivity*, **64**, (2003), 195-203.
- [34] J. Justo, H. Evangelista and A.S. Paschoa, Direct determination of <sup>226</sup>Ra in NORM/TENORM matrices by gamma-spectrometry. *Journal of Radioanalytical and Nuclear Chemistry*, **269**, (2006), 733-737.
- [35] K. Debertin and R.G. Helmer, *Gamma and X-Ray Spectrometry with Semiconductor Detectors*, North Holland: New York, (1988), Chapter 6.
- [36] M.U. Khandaker, High-purity germanium detector in gamma-ray spectrometry, *International Journal of Fundamental Physical Sciences*, **1**, (2011), 42 - 46.
- [37] P. Bode, E.A. Fernandes and R.R. Greenberg, Metrology for chemical measurements and the position of INAA, *Journal of Radioanalytical and Nuclear Chemistry*, **245**, (2000), 109 - 101.
- [38] M.A. Bacchi, E.A.N. Fernandes and H. Oliveira, A Brazilian experience on k0 standardized neutron activation analysis, *Journal of Radioanalytical and Nuclear Chemistry*, **245**, (2000), 217-222.
- [39] J. Crank, *The Mathematics of Diffusion*, Oxford: Clarendon Press, (1956).
- [40] D.A. Mineyev, Geochemical differentiation of the rare earths. *Geochemistry*, **12**, (1963), 1129-1149.
- [41] D.Z. Piper, Rare earth elements in the sedimentary cycle: a summary, *Chem. Geology*, **14**, (1974), 285-304.
- [42] G.D. Kaniyas and S.M. Philianos, Neutron activation analysis of distribution of certain elements between plant and soil, *Journal of Radioanalytical Chemistry*, **52**, (1979), 389-397.
- [43] B.E. Kogo, E.N. Gajere, J.K. Ogunmola and J.O. Ogbole, Neutron activation analysis of soil samples from different parts of Abuja Metropolis. *Middle-East Journal of Scientific Research*, **4**, (2009), 254-262.
- [44] A.A. Essiet, E.J. Uwat and S.O. Uwak, Elemental analysis of soil around Ikot Abasi aluminum smelter plant, Nigeria by Instrumental Neutron Analysis (INAA), *Scholars Research Library*, **3**, (2011), 25-32.
- [45] L.A. Haskin, F.A. Frey, R.A. Schmiti and R.H. Smith, Meteoritic, solar and terrestrial rare distributions, *Phys. Chem. Earth*, **7**, (1966), 169-321.
- [46] E. Anders and N. Grevesse, Abundances of the elements: Meteoric and solar, *Geochimica et Cosmochimica Acta*, **53**, (1989), 197-214.